1,3-Dipolar Cycloadditions of Electrophilically Activated Benzonitrile N-Oxides. Polar Cycloaddition versus Oxime Formation

ARTICLE *in* THE JOURNAL OF ORGANIC CHEMISTRY · JANUARY 2007

Impact Factor: 4.72 · DOI: 10.1021/jo0613986 · Source: PubMed

4 AUTHORS, INCLUDING:

Luis Ramon Domingo
University of Valencia
280 PUBLICATIONS **5,801** CITATIONS
SEE PROFILE

Pau Arroyo-Mañez
University of Buenos Aires
23 PUBLICATIONS **349** CITATIONS
SEE PROFILE

Jose Antonio Sáez Cases
Universitat Politècnica de València
50 PUBLICATIONS **980** CITATIONS
SEE PROFILE

JOC Article

1,3-Dipolar Cycloadditions of Electrophilically Activated Benzonitrile N-Oxides. Polar Cycloaddition versus Oxime Formation

Luis R. Domingo,* M. Teresa Picher, Pau Arroyo, and José A. Sáez

Departamento de Química Orgánica, Universidad de Valencia, Dr. Moliner 50, 46100 Burjassot, Valencia, Spain

domingo@utopia.uv.es

Received July 5, 2006

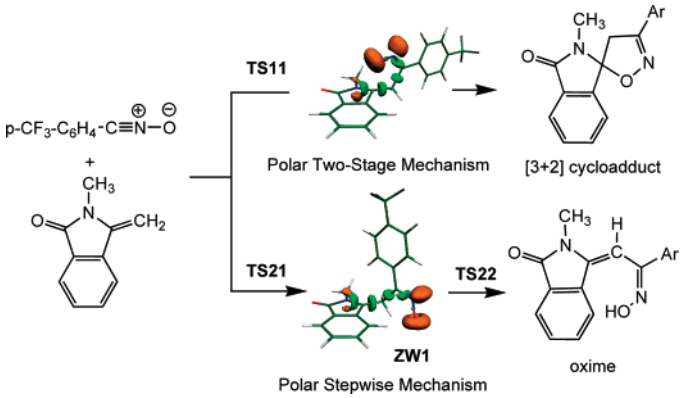

The reactions of electrophilically activated benzonitrile N-oxides (BNOs) toward 3-methylenephthalimidines (MPIs) have been studied using density functional theory (DFT) at the B3LYP/6-31G* level. For these reactions, two different channels allowing the formation of the [3 + 2] cycloadducts and two isomeric (*E*)- and (*Z*)-oximes have been characterized. The 1,3-dipolar cycloadditions take place along concerted but highly asynchronous transition states, while formation of the oximes is achieved through a stepwise mechanism involving zwitterionic intermediates. Both reactions are initiated by the nucleophilic attack of the methylene carbon of the MPIs to the carbon atom of the electrophilically activated BNOs. The analysis based on the natural bond orbital (NBO) and the topological analysis of the electron localization function (ELF) at the transition structures and intermediates explains correctly the polar nature of these reactions. Solvent effects considered by the PCM model allow explaining the low incidence of the solvent polarity on the rate and composition of the reactions.

Introduction

Cycloaddition reactions are one of the most important processes, with both synthetic and mechanistic interest in organic chemistry. Current understanding of the underlying principles in the Diels−Alder (DA) reactions[1] and the 1,3-dipolar cycloaddition (13DC) reactions[2] has grown from a fruitful interplay between theory and experiment. The general concept of 13DC was introduced by Huisgen and co-workers in the early 1960s.[3] Huisgen's work stated the basis for the understanding of the mechanism of concerted cycloaddition reactions. Given the importance of these reactions, a strong effort has been directed toward the characterization of the reagents in these cycloadditions as well as the elucidation of its reaction mechanism.[4] However, the nature of the 13DC reaction mechanism is still an open problem in physical organic chemistry. For instance, the mechanism proposed by Huisgen's group is that of a single-step, four-center cycloaddition, in which two new bonds are both partially formed at the transition state, although not necessarily to the same extent.[5] For nitrile N-oxide (RCNO) cycloadditions, experimental data were interpreted as either

(1) Wasserman, A. *Diels−Alder Reactions*; Elsevier: New York, 1965.
(2) Padwa, A. *1,3-Dipolar Cycloaddition Chemistry*; Wiley-Interscience: New York, 1984; Vols. 1−2.
(3) Huisgen, R.; Grashey, R.; Sauer, J. *The Chemistry of Alkenes*; Interscience: New York, 1964.
(4) Huisgen, R. *1,3-Dipolar Cycloaddition Chemistry*; Wiley: New York, 1984; Vol. 1.
(5) (a) Huisgen, R. *J. Org. Chem.* **1968**, *33*, 2291−2297. (b) Huisgen, R. *J. Org. Chem.* **1976**, *41*, 1976−1979.

10.1021/jo0613986 CCC: $33.50
Published on Web 11/15/2006

SCHEME 1

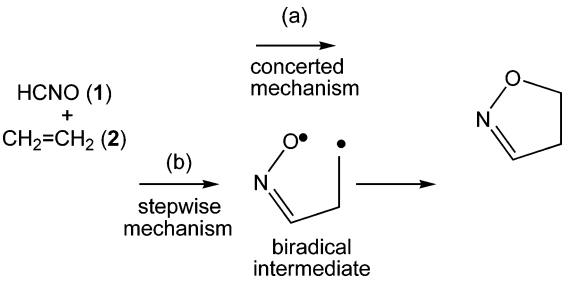

SCHEME 2

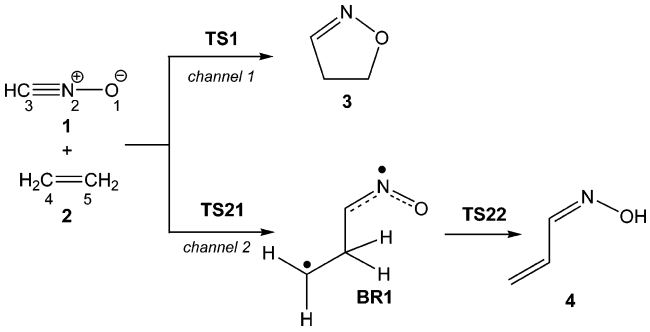

being consistent with a concerted mechanism (mechanism a in Scheme 1)[5] or in favor of a stepwise mechanism with biradical (BR) intermediates (mechanism b in Scheme 1).[6]

The mechanisms of the 13DC reactions of the simplest nitrile N-oxide, fulminic acid (HCNO, **1**), as the dipole component have been widely studied from a theoretical point of view in order to the elucidate their concerted or BR stepwise nature of its mechanism.[7] In 1983, Schelegel et al.[7b] studied the 13DC of fulminic acid **1** with acetylene at the UHF level. They proposed that the barrier for the Firestone radical mechanism was 3.6 kcal/mol lower in energy than that for the Huisgen concerted one. However, the low energy difference seemed to indicate that both mechanisms could be competitive. A further study carried out at the MCSCF level[7c] indicated that the concerted mechanism was slightly lower in energy than the BR stepwise one. A similar trend was found for the 13DC reaction between fulminic acid **1** and ethylene **2** (see Scheme 2). The MCSCF/4-31G energy barrier associated with the formation of the BR intermediate, **BR1**, was found to be 8.4 kcal/mol higher in energy than that associated with the concerted process, which leads to the formation of the [3 + 2] cycloadduct **3**. In addition, the transition structure (TS) associated with the hydrogen

SCHEME 3

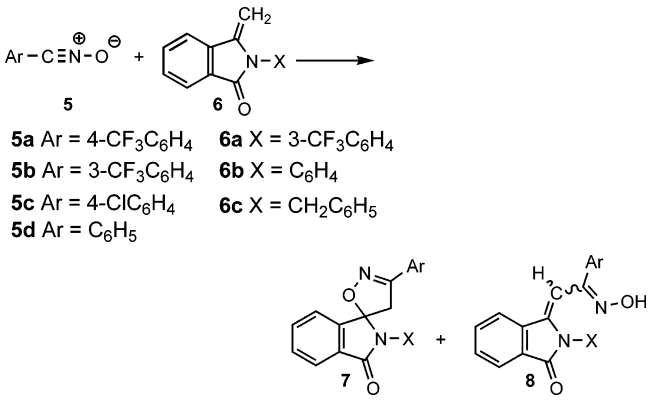

transfer process with formation of the corresponding oxime **4** was 39.5 kcal/mol over the reactants (see Scheme 2).

The 13DC reaction between fulminic acid **1** and acetylene was more recently studied by Nguyen et al.[7f] using methods that include dynamical electron correlation in order to obtain accurate energy barriers. These authors found that both CCSD-(T) and CASPT2 results agree each other, suggesting that the energy barrier associated with the concerted mechanism is about 14 kcal/mol. A closer energetic result was obtained at the B3LYP/6-31G* level, 13.4 kcal/mol. For the 13DC reaction between fulminic acid **1** and ethylene **2**, the energy barrier of the concerted mechanism has been estimated to be 11.4 kcal/mol at the B3LYP/6-31G* level.[7d]

Recently, the reaction between fulminic acid **1** and acetylene has been studied in terms of the electron localization function (ELF) and the catastrophe theory.[7m] The analysis of the basin population calculated with the ELF along the IRC for the concerted mechanism suggests that the reaction is a two-stage process in which the O−C bond formation is initiated after the complete C−C bond formation. At the TS geometry, the ELF analysis indicates that at this stage of the reaction only the C−C is being formed.[7m]

In 1990, Howe and Shelton[8] reported the reactions of several benzonitrile N-oxides (BNO, **5**) with 3-methylenephthalimidines (MPI, **6**) (see Scheme 3). For the reactions of BNOs **5a**−**c** with the MPI **6c**, together with the main product of the reactions, a spiroheterocycle (**7**), two stereoisomeric (*E*)- and (*Z*)-oximes (**8**) were also obtained. The oximes **8** were not observed for the reactions of **5** with **6a** and **6b**. The low solvent effects on the reaction rate and on the product ratio for the reactions of **5b** induced these authors to suggest that the product mixture resulted from a competition between a 13DC reaction to give the [3 + 2] cycloadduct **7** and a stepwise BR reaction to give the oximes **8** (see Scheme 4).

Some papers have reported the oxime formation on the reactions of some nitrile N-oxides with specific dipolarophiles as furans,[9a] indenes,[9b] and uracil derivatives.[9c] Most of them involve electrophilically activated nitrile N-oxides. Very recently, Tsoleridis et al.[10] have reported an experimental and theoretical study for the reactivity and regioselectivity of the reaction of indole *o*-quinodimethanes **9** toward the BNOs **5e**,**f**

(6) (a) Firestone, R. A. *J. Org. Chem.* **1968**, *33*, 2285−2290. (b) Firestone, R. A. *J. Org. Chem.* **1972**, *37*, 2181−2191.

(7) (a) Poppinger, D. *J. Am. Chem. Soc.* **1975**, *97*, 7486−7488. (b) Hiberty, P. C.; Ohanessian, G.; Schlegel, H. B. *J. Am. Chem. Soc.* **1983**, *105*, 719−723. (c) McDouall, J. J. W.; Robb, M. A.; Niazi, U.; Bernardi, F.; Schlegel, H. B. *J. Am. Chem. Soc.* **1987**, *109*, 4642−4648. (d) Rastelli, A.; Gandolfi, R.; Sarzi-Amadé, M. *J. Org. Chem.* **1998**, *63*, 7425−7436. (e) Magnuson, E. C.; Pranata, J. *J. Comput. Chem.* **1998**, *19*, 1795−1804. (f) Nguyen, M. T.; Chandra, A. K.; Sakai, S.; Morokuma, K. *J. Org. Chem.* **1999**, *64*, 65−64. (g) Su, M. D.; Liao, H. Y.; Chung, W. S.; Chu, S. Y. *J. Org. Chem.* **1999**, *64*, 6710−6716. (h) Cossío, F. P.; Morao, I.; Jiao, H.; Schleyer, P. v. R. *J. Am. Chem. Soc.* **1999**, *121*, 6737−6746. (i) Sakata, K. *J. Phys. Chem. A* **2000**, *104*, 10001−10008. (j) Nguyen, M. T.; Chandra, A. K.; Uchimaru, T.; Sakai, S. *J. Phys. Chem. A* **2001**, *105*, 10943−10945. (k) Sakai, S.; Nguyen, M. T. *J. Phys. Chem. A* **2004**, *108*, 9169−9179. (l) Vullo, V.; Danks, T.; Wagner, G. *Eur. J. Org. Chem.* **2004**, 2046−2052. (m) Polo, V.; Andrés, J.; Castillo, R.; Berski, S.; Silvi, B. *Chem.—Eur. J.* **2004**, *10*, 5165−5172. (n) Kavitha, K.; Venuvanalingam, P. *Int. J. Quantum Chem.* **2005**, *104*, 64−78.

(8) Howe, R. K.; Shelton, B. R. *J. Org. Chem.* **1990**, *55*, 4603−4607.

(9) (a) Caramella, P.; Cellerino, G.; Corsico, A.; Gamba, A; Grunanger, P.; Houk, K. N. Marinone, F. *J. Org. Chem.* **1976**, *41*, 3349−3356. (b) Tanaka, K.; Masuda, H.; Mitsuhashi, K. *Bull. Chem. Soc. Jpn.* **1985**, *58*, 2061−2065. (c) Kim, J. N.; Ryu, E. K. *J. Org. Chem.* **1992**, *57*, 1088−1092.

SCHEME 4

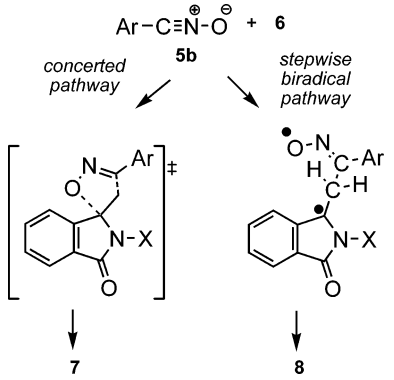

SCHEME 5

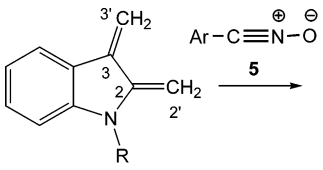

9a R = COPh
9b R= COMe
9c R = SO_2Ph
5e Ar = 2,6-$Cl_2C_6H_3$
5f Ar = 2,4,6-$Me_3C_6H_2$

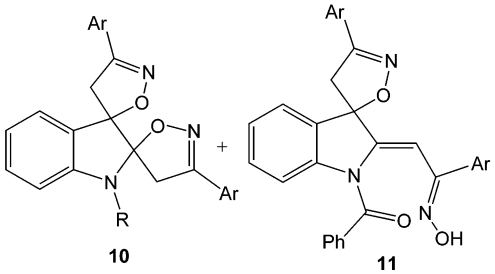

(see Scheme 5). The main products of the reaction were the corresponding [3 + 2] cycloadducts **10**, a dispiroisoxazolidines. When the electrophilically activated BNO **5f** was used, together with the [3 + 2] cycloadducts **10**, 13% of the oxime **11** was also isolated.[10] It is interesting to remark that, when the 2,4,6-trimethylbenzoylnitrile N-oxide **5f** was used, formation of the corresponding oxime was not observed. The selectivity of the cycloaddition was studied using AM1 semiempirical methods. Both analysis of the potential energy surface (PES) for the reaction, as well the FMO analysis on the indole *o*-quinodimethanes **9**, indicated that the reaction is initiated at the C2−C2′ double bond,[10] which presents an environment similar to that of the exocyclic methylene of the MPIs **6**.

The mechanisms of the reactions of electrophilically activated nitrile N-oxides with C−C double bonds with formation of oxazolidines and oximes have not been theoretically studied. In the present paper, the mechanisms of the reactions between BNOs and MPIs with formation of [3 + 2] cycloadducts and (*E*)- and (*Z*)-oximes reported by Howe and Shelton[8] have been studied in order to understand the electronic nature of these 13DC reactions, BR or zwitterionic (ZW), as well as the factors controlling the competitive formations of oximes.

Three reaction models have been selected: the first one, *Model I*, corresponds to the reaction between fulminic acid **1** and ethylene **2**. The BR nature of the species involved in the stepwise pathway with formation of the corresponding oxime **4** will be analyzed. Although the concerted mechanism has been recently studied at high level of theory,[7d,f,g,i−k,m] to the best of our knowledge, the BR stepwise mechanism has never been treated. Then, the reactions between the BNO **5a** and the MPI **6d** as a molecular model of **6c**, *Model II*, will be studied. Analysis of the bond order (BO), charge transfer (CT), and ELF at the TSs and intermediates involved in the formation of the [3 + 2] cycloadduct **12** and the (*E*)- and (*Z*)-oximes **13** will be performed in order to state the polar nature of these reactions. Finally, the *Model III* corresponds to the reaction of the BNO **5f** with acrolein **15** as a reaction model of those reactions involving electrophilically activated dipolarophiles. Both concerted and stepwise channels will be investigated in order to understand the non-formation of oximes in these kinds of cycloadditions. The electronic structure of TSs and intermediates involved in the three reaction models will be analyzed in order to characterize the electronic nature of these reactions: BR (nonpolar) or ZW (polar). In the last section, a DFT analysis based on the global reactivity indexes of the reactants involved in these 13DC reactions will be performed.

Computational Models

DFT calculations were carried out using the B3LYP exchange-correlation functionals, together with the standard 6-31G* basis set (see Supporting Information for computational details). For the reaction *Model I*, CCSD(T)[11] and BD(T)[12] single-point energy calculations were performed at the DFT-optimized structures. Recent studies devoted to reaction mechanisms involving BR intermediates have indicated that, while calculations performed at these theoretical levels provide reasonable energies, calculations performed at the CASSCF[13] level give large energies for the corresponding BR species.[7f,14]

The ELF was defined as a measure of the local Pauli repulsion, and its topological analysis provides us with a useful and convenient partitioning of the molecular space into regions that are associated with chemically meaningful concepts, such as atomic shells, bonds, and lone pairs. Each region, termed basin, is related to a local maximum (i.e., an attractor) of the ELF analysis, and it is interpreted as a region where it is likely to localize an electron or a pair of electrons. The basins are either core basins labeled C(A) or valence basins V(A,...) belonging to the outermost shell. Valence basins are characterized by their coordination number (the synaptic order) with the core. Hence, lone pairs are represented by monosynaptic basins, covalent bonding between two atoms by a disynaptic, and so on. This methodology has been well documented in a series of articles presenting its theoretical foundations.[15] A quantitative analysis is performed through the integration of the electronic density $\rho(r)$ in the volume of the ELF basin, Ω. The integrated basin population (N_i) of a given basin is calculated

$$N_i = \int_{\Omega_i} \rho(r)\mathrm{d}r \qquad (1)$$

Following the N_i along a calculated reaction path is a useful technique that allows on to identify the specific flows of the

(10) Tsoleridis, C. A.; Dimtsas, J.; Hatzimimikou, D.; Stephanidou-Stephanatou, J. *Tetrahedron* **2006**, *62*, 4243−4242.

(11) (a) Purvis, G. D.; Bartlett, R. J. *J. Chem. Phys.* **1982**, *76*, 1910−1918. (b) Scuseria, G. E.; Janssen, C. L.; Schaefer, H. F., III. *J. Chem. Phys.* **1998**, *89*, 7382−7387. (c) Seerden, J.-P. G.; Scholte op Reimer, A. W. A.; Scheeren, H. W. *Tetrahedron Lett.* **1994**, *35*, 4419−4422.

(12) Handy, N. C.; Pople, J. A.; Head-Gordon, M.; Raghavachari, K.; Trucks, G. W. *Chem. Phys. Lett.* **1989**, *164*, 185−192.

(13) (a) Roos, B. O.; Taylor, P. R. *Chem. Phys.* **1980**, *48*, 157−173.

(14) (a) Navarro-Váquez, A.; Prall, M.; Schreiner, P. R. *Org. Lett.* **2004**, *6*, 2981−2984. (b) Schreiner, P. R.; Navarro-Vázquez, A.; Prall, M. *Acc. Chem. Res.* **2005**, *38*, 29−37. (c) Domingo, L. R.; Pérez-Prieto, J. *ChemPhysChem* **2006**, *7*, 614−618.

TABLE 1. UB3LYP/6-31G*, CCSD(T)/6-31G*, and BD(T)/6-31G* Relative Energies (ΔE, in kcal/mol, relative to 1 + 2) of the Stationary Points for the Concerted and Stepwise Reactions between Fulminic Acid 1 and Ethylene 2

	UB3LYP	CCSD(T)	BD(T)
TS1	11.3	11.0	11.1
3	−45.9	−49.2	−49.4
TS21	18.9	19.6	19.9
BR1	8.2	13.2	12.3
TS22	17.4	22.2	21.7
4	−26.1	−29.0	−29.2

electronic charge occurring along a chemical reaction and provides a rational characterization of chemical concepts such as bond forming/breaking process, obtaining new insights on the reaction mechanism. ELF analysis was carried out using a cubical grid of step size smaller than 0.1 bohr employing the TopMod[16] package of programs.

Results and Discussions

(a) Study of the Reaction between Fulminic Acid 1 and Ethylene 2. Concerted versus Biradical Stepwise Mechanism. Reaction Model I. For the reaction between fulminic acid **1** and ethylene **2**, reaction *Model I*, two channels have been studied: the concerted and the stepwise one (see Scheme 2). They are related to the N2−C3−C4−C5 dihedral angle formed by the N2−C3 and C4−C5 π-bonds along the approach of the two molecules: 0 and 120°. Along the 0° approach mode, *channel 1*, both C−C and O−C new σ-bonds are formed in a concerted fashion to give the corresponding [3 + 2] cycloadduct. However, along the 120° approach mode, *channel 2*, only the C−C σ-bond formation is feasible, yielding a BR intermediate.[7c] A further C−C bond rotation or hydrogen abstraction converts this intermediate in the [3 + 2] cycloadduct or in the oxime through a stepwise process. Therefore, three TSs, **TS1**, **TS21** and **TS22**, one BR intermediate, **BR1**, and two products, the [3 + 2] cycloadduct **3** and the oxime **4**, have been located and characterized (see Scheme 2).

The activation energy associated with the formation of the [3 + 2] cycloadduct **3** via the concerted pathway is 11.3 kcal/mol (**TS1**) (see Table 1).[7g] Formation of the corresponding cycloadduct is strongly exothermic, −45.9 kcal/mol. These relative energies are closer to those obtained by single-point energy calculations at the very high computing demand CCSD-(T)/6-311G** level.[7g] For the stepwise pathway, the activation energy associated with the attack of ethylene **2** to fulminic acid **1** with formation of the intermediate **BR1** is 18.9 kcal/mol (**TS21**). The intermediate **BR1** is located 8.2 kcal/mol above the reagents. The activation energy associated with the hydrogen abstraction at the intermediate **BR1** with formation of the oxime **4** is 9.2 kcal/mol (**TS22**). Formation of the oxime is exothermic in −26.1 kcal/mol. These energetic results show that the TS associated with the attack of ethylene to fulminic acid along the stepwise pathway, **TS21**, is 7.6 kcal/mol higher in energy than that associated with concerted one, **TS1**. This large energy difference prevents either 13DC reaction or the oxime formation through the BR stepwise mechanism.

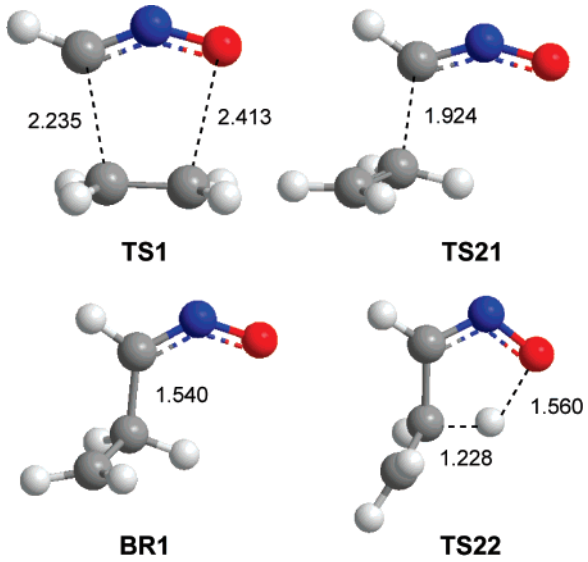

FIGURE 1. Structures of the transition states and biradical intermediate involved in the concerted and stepwise reaction pathways between fulminic acid **1** and ethylene **2**, reaction *Model I*. The distances are given in angstroms.

In order to validate the DFT energies, CCSD(T) and BD(T) single-point energy calculations were performed (see Table 1). The B3LYP activation energies associated with the concerted 13DC reaction and the formation of the intermediate **BR1** agree closely with those obtained at the CCSD(T)and BD(T) levels: ca. 11 and 19 kcal/mol. Formation of the **BR1** intermediate is ca. 8 kcal/mol more energetic than the concerted formation of the [3 + 2] cycloadduct **3**; the BR stepwise mechanism is clearly not favored. B3LYP calculations underestimate the energies of the intermediate **BR1** and **TS22** by ca. 5 kcal/mol. The activation energy for the hydrogen transfer process at the three computational methods is ca. 9 kcal/mol. Finally, B3LYP calculations underestimate the energy of formation of the [3 + 2] cycloadduct **3** and the oxime **4** by ca. 4 kcal/mol.

The lengths of the forming bonds at the TSs and the BR intermediate are given in Figure 1. The N2−C3−C4−C5 dihedral angles at **TS1** and **TS21** that define the approach mode of ethylene to fulminic acid are 0.0 and 125.0°. The N2−C3−H3 bond angles at **TS1**, **TS21**, and **BR1** of 136.4, 128.3, and 116.8°, respectively, show the change from an sp to an sp^2 hybridization of the C3 atom of the nitrile N-oxide.

The electronic structures of the TSs and the intermediate involved in the reaction between fulminic acid **1** and ethylene **2** were analyzed using the Wiberg bond order[17] (BO) values, the natural population analysis (NPA), and the analysis of the Mulliken spin electron density. At the concerted **TS1**, the BO values of the C3−C4 and O1−C5 forming bonds, 0.45 and 0.12, point out a high asynchronous bond formation. At **TS21**, the BO value of the C3−C4 forming bond is 0.48, while this value at **BR1** is 0.95. Finally, at **TS22**, the BO values at the C4−H4 breaking and O1−H4 forming bonds are 0.59 and 0.22.

The NPA allows us to evaluate the CT along the attack of ethylene **2** to fulminic acid **1**. The natural charges at the **TS1**, **TS21**, and **BR1** have been shared between fulminic acid and ethylene frameworks. The sum of the natural charges at the fulminic acid framework at these species is 0.02 e (**TS1**),

(15) (a) Savin, A.; Becke, A. D.; Flad, J.; Nesper, R.; Preuss, H.; Vonschnering, H. G. *Angew. Chem., Int. Ed. Engl.* **1991**, *30*, 409−412. (b) Silvi, B.; Savin, A. *Nature* **1994**, *371*, 683−686.

(16) Noury, S.; Krokidis, X.; Fuster, F.; Silvi, B. *Comput. Chem.* **1999**, *23*, 597−604.

(17) Wiberg, K. B. *Tetrahedron* **1968**, *24*, 1083−1096.

SCHEME 6

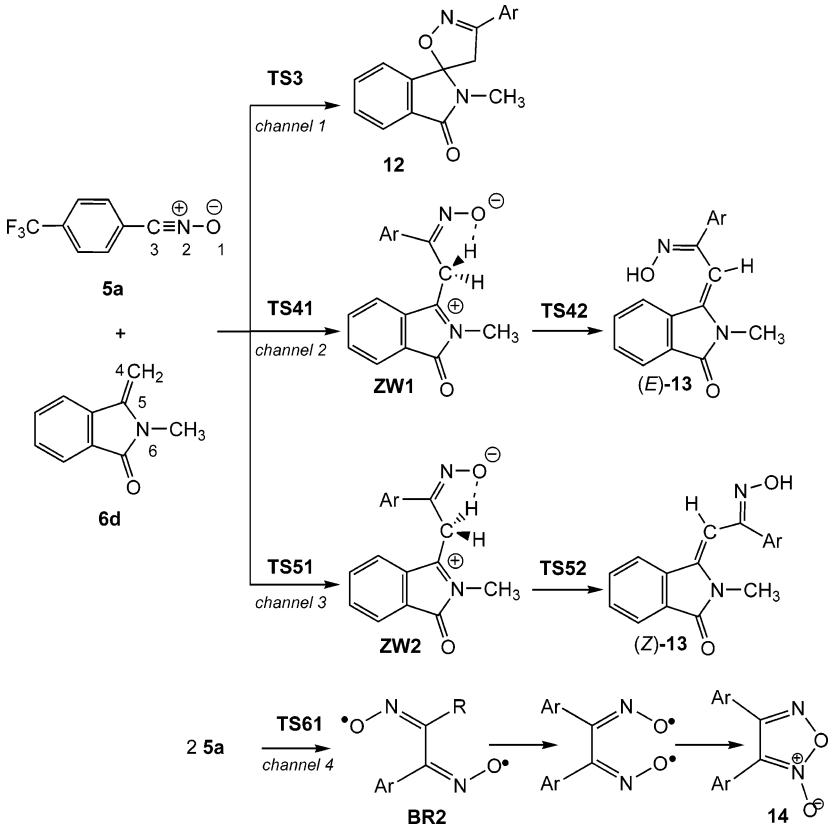

0.09 e (**TS21**), and 0.03 e (**BR1**). These very low values point to the nonpolar character of these processes.

The TSs and intermediate involved at the stepwise mechanism have a BR character. Initial $<S^2>$ values for the singlet BR stationary points, 0.26 (**TS21**), 0.90 (**BR1**), and 0.31 (**TS22**), become 0.01 (**TS21**), 0.07 (**BR1**), and 0.01 (**TS22**) after spin annihilation.[18] At the intermediate **BR1**, the atomic spin density is mainly located at O1 (−0.52), N2 (−0.40), and C5 (1.01). These values indicate that the electronic structure of this intermediate is in agreement with a BR specie where one α electron is mainly delocated at the O1 and N2 atoms belonging to the fulminic acid residue, while the second β electron is localized on the terminal C5 atom belonging to the ethylene residue.

A complete analysis of the topology of the ELF for the 13DC reaction between fulminic acid **1** and acetylene has been recently done.[7m] The topology of the ELF of **TS1**, **TS21**, and the intermediate **BR1** was studied in order to analyze the CT at these species. The amount of CT on these processes has been evaluated by adding the core and valence basins belonging to the fulminic acid and ethylene fragments. This sum at the fulminic acid framework is 15.90 e at **TS1**, 15.85 e at **TS21**, and 16.00 e at **BR1**. The negligible deviation of these values with regard to that at the fumaric acid **1**, 16.00 e, allows us to assert the nonpolar nature of these processes. At the intermediate **BR1**, the CT is 0.00 e, in clear agreement with the CT analysis based on the natural charges.

(b) Study of the Mechanisms Involved in the Reaction between 4-(Trifluoromethyl)benzonitrile N-Oxide 5a and 2-Methyl-3-methylenephthalimidines 6d. Polar Mechanism.

(18) Cramer, C. J.; Dulles, F. J.; Giesen, D. J.; Almlöf, J. *Chem. Phys. Lett.* **1995**, *245*, 165−170.

Reaction Model II. As was mentioned in the Introduction, the reactions between the BNOs **5a**−**c** and the MPI **6c** yield mainly spirocycloadducts, [3 + 2] cycloadducts, and in a minor ratio mixture of two (*E*)- and (*Z*)-oximes (see Scheme 3).[8] Therefore, the reaction pathways connecting the BNO **5a** and the MPI **6d** with the formation of the [3 + 2] cycloadduct **12** and the oximes (*E*)-**13** and (*Z*)-**13** were investigated as model of these reactions (see Scheme 6). Three channels were studied. They are related to the dihedral angle formed between the π C−N bond of BNO and the π C−C bond of MPI along the C−C bond formation, which take the values of 0, 120, and 240°. These channels are named as *channel 1* (0°), *2* (120°), and *3* (240°), allowing the concerted formation of the [3 + 2] cycloadduct **12** and the stepwise formation of the oximes (*E*)-**13** and (*Z*)-**13**, respectively. Thus, five TSs, **TS3**, **TS41**, **TS51**, **TS42**, and **TS52**, two ZW intermediates, **ZW1** and **ZW2**, one [3 + 2] cycloadduct, **12**, and two oximes, (*E*)-**13** and (*Z*)-**13**, were located and characterized (see Scheme 6).

The activation energy associated with the formation of the [3 + 2] cycloadduct **12** via the concerted pathway is 13.5 kcal/mol (**TS3**) (see Table 2). This energy is slightly larger than that obtained for the 13DC reaction between fulminic acid **1** and ethylene **2**. Formation of the corresponding cycloadduct is exothermic at −35.4 kcal/mol. For the stepwise pathways, the activation energy associated with the attack of the MPI **5a** to the BNO **6d** with formation of the intermediates **ZW1** and **ZW2** is 14.2 kcal/mol (**TS41**) and 14.0 kcal/mol (**TS51**). The intermediates **ZW1** and **ZW2** are located 3.7 and 3.4 kcal/mol above the reagents. The activation energy associated with the proton abstraction at the intermediates **ZW1** and **ZW2** with formation of the oximes (*E*)-**13** and (*Z*)-**13** is 1.7 kcal/mol (**TS42**) and 1.4 kcal/mol (**TS52**). Formation of the oximes (*E*)-

TABLE 2. (U)B3LYP/6-31G* Relative Energies (Δ*E*, in kcal/mol, relative to 5a + 6d or 5a + 5a), in the Gas Phase and in Dichloromethane, of the Stationary Points for Concerted and Stepwise Reactions between the Benzonitrile N-Oxide 5a and 3-Methylenephthalimidines 6d, and the First Step of the Dimerization of 5a

	gas phase	dichloromethane
TS3	13.5	14.7
12	−35.4	−34.6
TS41	14.2	16.6
ZW1	3.7	3.5
TS42	5.4	6.0
(*E*)-13	−21.2	−20.4
TS51	14.0	16.1
ZW2	3.4	2.4
TS52	4.8	5.9
(*Z*)-13	−20.5	−20.1
TS61	16.3	19.3
BR2	−7.6	−3.2

13 and (*Z*)-**13** is exothermic by −21.2 and −20.5 kcal/mol. Unlike the reaction between fulminic acid **1** and ethylene **2**, the concerted and stepwise channels associated with the reaction between the BNO **5a** and MPI **6b** are competitive. In addition, the low activation energy associated with the proton transfer process favors this way over the ring closure to give the [3 + 2] cycloadduct **12**.

Formation of the [3 + 2] cycloadduct **12** is thermodynamically favored over formation of the oximes **13** by ca. 14−15 kcal/mol. These large energies together with the strong exothermic character of three competitive channels prevent the equilibration between these species and, as a consequence, the isomerization of **12** to **13**. Note that the activation energy associated with the ring opening of the [3 + 2] cycloadduct **12** is 48.9 kcal/mol, whereas the zwitterionic intermediates are located 39 kcal/mol above the [3 + 2] cycloadduct **12**. Therefore, under the experimental conditions (room temperature), it is expected that the oxime formation via a ring opening process of the [3 + 2] cycloadduct **12** will not be operative as was remarked by Howe and Shelton.[8] Note that these DFT thermodynamic results are closer to those obtained for the formation of the [3 + 2] cycloadduct **3** and the oximes **4** at the CCSD(T) and BD(T) levels (see Table 1).

The lengths of the forming bonds at the TSs and intermediates are given in Figure 2. The extent of the asynchronicity on the bond formation at the concerted **TS3** is $\Delta r_{[d(O1-C5)-d(C3-C4)]} = 0.49$. This value, which is larger than that associated with **TS1**, $\Delta r = 0.22$, indicates that **TS3** corresponds to an asynchronous concerted bond formation process, where the C3−C4 bond is being formed in an extension larger than the O1−C5 one. The N2−C3−C4−C5 dihedral angles at **TS3**, **TS41**, and **TS51** are 6.0, 112.2, and −105.0°, respectively. At **ZW1** and **ZW2**, the distances between the O1 and H4 atoms, 1.912 and 1.868 Å, point out the formation of a hydrogen bond between the H3 hydrogen and the O1 oxygen atoms. This distance at the intermediate **BR1** is 2.526 Å.

The IRC calculations from the concerted **TS3** show that the *channel 1* directly connects this TS with the [3 + 2] cycloadduct **12**, without the participation of any intermediate. Analysis of the points along the IRCs shows that this 13DC cycloaddition is a concerted two-stage process.[19] In the first stage, the C3−C4 bond is completely formed through the nucleophilic attack of the C4 position of the MPI **6d** to the C3 carbon atom of the BNO **5a**. The O1−C5 bond is formed in the second stage of the reaction. From the IRC of **TS3** to the cycloadduct **12**, we have selected the "halfway" point, **HWP**,[20] which shares the reaction coordinates in the two stages (Figure 2). At this point of the IRC, the asynchronicity on the bond formation, $\Delta r = 0.73$, is larger than that at the corresponding **TS3**.

At the concerted **TS3**, the BO values of the C3−C4 and O1−C5 forming bonds, 0.31 and 0.11, indicate that this TS corresponds to an asynchronous bond formation process. At **HWP**, the C3−C4 BO value, 0.93, indicates that this bond is already formed, while the BO value between the O1 and C5 atoms remains at 0.38. At **TS41** and **TS51**, the BO values of the C3−C4 forming bonds are 0.39 and 0.42, while those values at the intermediates **ZW1** and **ZW2** are 0.89 and 0.90. At these intermediates, the C5−N6 BO values, 1.23 and 1.24, point to a π-character of the C5−N6 bond as a consequence of the delocalization of the lone pair of the amide N6 nitrogen atom on the C4−C5 framework. Finally, at **TS42** and **TS52**, the BO values at the C4−H4 breaking and O1−H4 forming bonds are 0.57 and 0.25, and 0.57 and 0.25, respectively.

The NPA allows us to evaluate the CT along the attack of the MPI **6d** to the BNO **5a**. The natural charges at the **TS3**, **TS41**, **TS51**, **ZW1**, and **ZW2** have been shared between BNO and MPI frameworks. The CT that fluxes from MPI to BNO at these species is 0.07 e (**TS3**), 0.14 e (**TS41**), 0.14 e, (**TS51**), 0.40 e (**ZW1**), and 0.40 e (**ZW2**). At the **TS3**, **TS41**, and **TS51**, there is a low CT. However, along the stepwise pathways there is an increase of the CT until formation of the intermediates **ZW1** and **ZW2**. Note that at the BR intermediate **BR1** the CT is negligible, 0.03 e. These results are in agreement with the increase of the dipole moment of these species going from TSs to intermediates: 1.57 D at **TS41**, 5.10 D at **ZW1**, 3.93 D at **TS51**, and 6.94 D at **ZW2**. At the BR stepwise process, there is a decrease on the dipole moment from 3.27 D at **TS21** to 2.79 D at **BR1**. The **HWP** presents a CT, 0.30 e, closer to that at the ZW intermediates. Therefore, although the concerted **TS3** presents a low CT, along the reaction channel, the CT increases to the complete C3−C4 bond formation. These results point out the polar nature of these cycloadditions.

As some species involved in the reaction have some ZW character, solvent effects of dichloromethane were evaluated. In dichloromethane, all species are stabilized between 3 and 12 kcal/mol. The most stabilized species are the intermediates **ZW1** and **ZW2** and the TSs involved in the proton transfer process, **TS42** and **TS52**, in clear agreement with the ZW character of these species. For the concerted process, the activation energy increases slightly to 1.2 kcal/mol as a consequence of a larger solvation of the reagents than **TS3** (see Table 2). In addition, although the ZW intermediates are the most stabilized species, the TSs associated with their formation are less stabilized than the concerted TS; as a consequence, the relative energies of these TSs increase from 0.8 kcal/mol in the gas phase to 1.9 kcal/mol in dichloromethane. Finally, in dichloromethane, the TS associated with the formation of the (*Z*)-isomer, **TS51**, is slightly more stabilized than that associated with the formation of the (*E*)-isomer, **TS41** (0.5 kcal/mol). The energy results obtained with the inclusion of the solvent effect are in reasonable agreement with the low solvent effect found by Howe and Shelton,[8] despite the ZW nature of these reactions. Inclusion of solvent effects on the geometrical optimization by

(19) Dewar, M. J. S.; Olivella, S.; Stewart, J. J. P. *J. Am. Chem. Soc.* **1986**, *108*, 5771−5779.

(20) Domingo, L. R. *J. Org. Chem.* **2001**, *66*, 3211−3214.

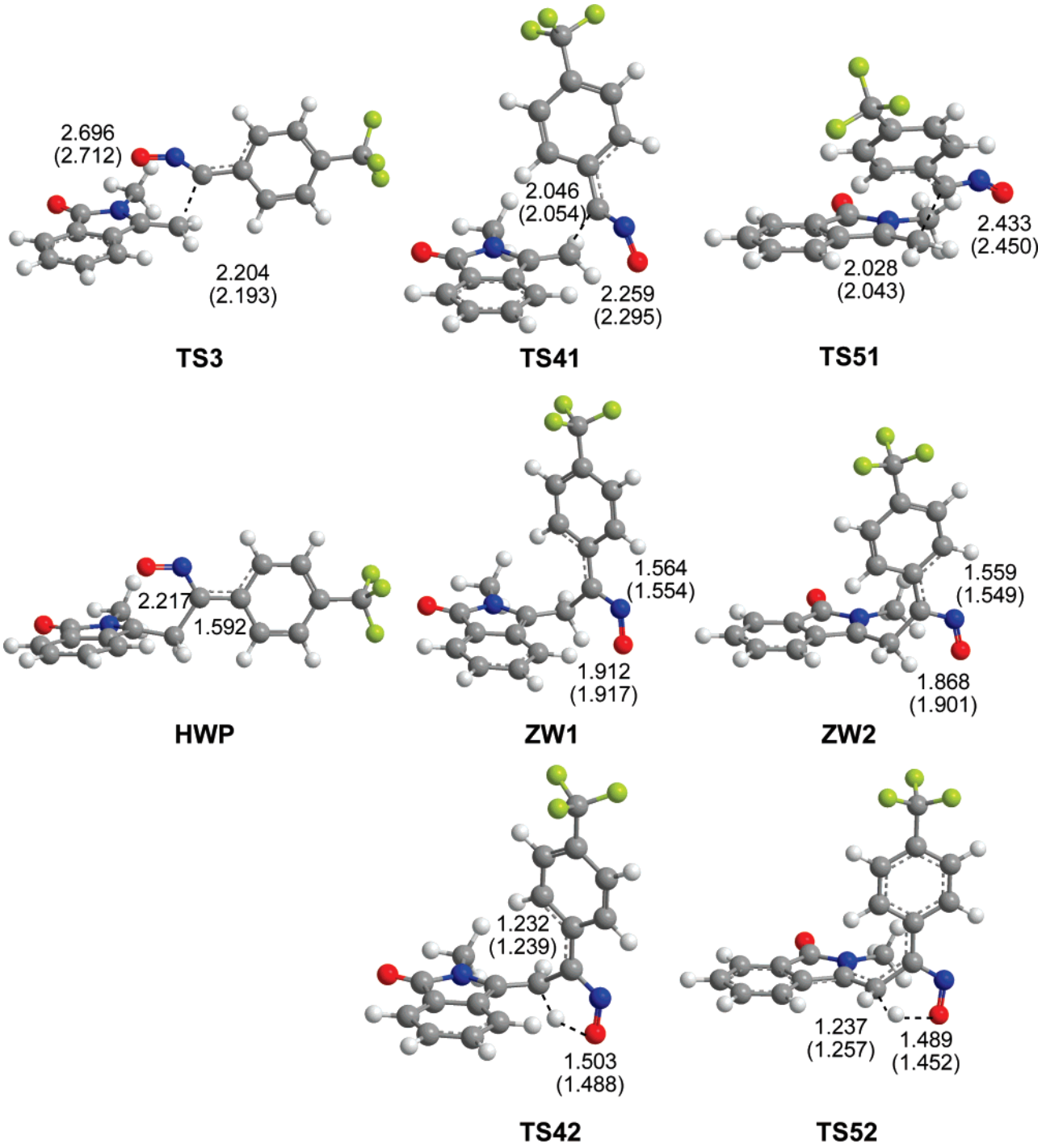

FIGURE 2. Structures of the transition states and zwitterionic intermediates involved in the concerted and stepwise reaction pathways between 4-trifluoromethylbenzonitrile N-oxide **5a** and 3-methylenephthalimidine **6d**, reaction *Model II*. The geometry of the IRC point **HWP** is also given. The distances are given in angstroms. Values in parentheses correspond to the geometries in dichloromethane.

the PCM approach does not modify substantially the gas phase geometries (see Figure 2). The variations of the lengths of the forming bonds at the TSs and intermediates are less than 0.04 Å.

In addition to the 13DC reaction and the oxime formation, dimerization of the nitrile N-oxides to form 1,2,5-oxadiazole-2-oxides (**14**), commonly known as furoxans, is also feasible (see *channel 4* in Scheme 6). Howe and Shelton indicated that a minor amount of dimerization of the BNOs **5** competed with the reactions with **6**.[8] As a consequence, this competitive reaction for **5a** has been also considered. Dimerization of nitrile N-oxides, including 4-chlorobenzonitrile N-oxide **5c**, has been studied recently by Houk et al.[21] They found that these reactions are stepwise processes involving BR intermediates. The UB3LYP/6-31G* activation energies for the first and rate-determining

(21) (a) Yu, Z.-X.; Caramella, P.; Houk, K. N. *J. Am. Chem. Soc.* **2003**, *125*, 15420−15425. (b) Yu, Z.-X.; Houk, K. N. *J. Am. Chem. Soc.* **2003**, *125*, 13825−13830.

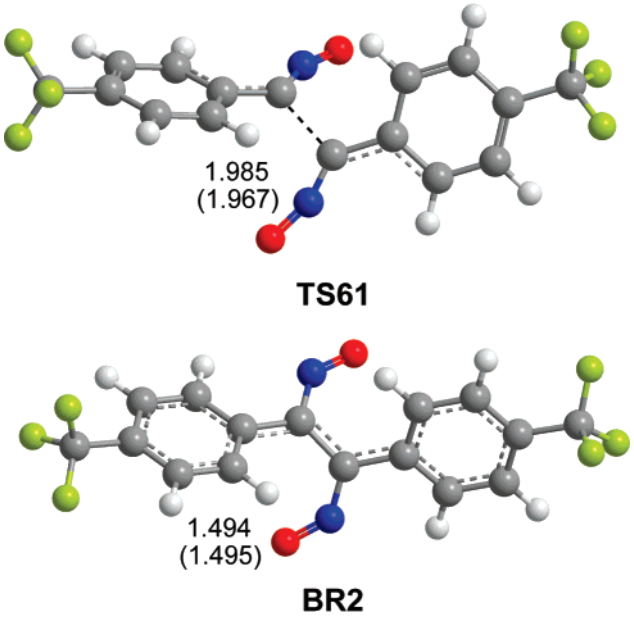

FIGURE 3. Structures of the transition state and biradical intermediate involved in the first step of the dimerization reaction pathway of 4-trifluoromethylbenzonitrile N-oxide **5a**. The distances are given in angstroms. Values in parentheses correspond to the geometries in dichloromethane.

steps were between 11.1 and 14.2 kcal/mol. The larger energy, which corresponds to the dimerization of aromatic BNO **5c**, was attributed to the reduction of the conjugation between the phenyl and the CNO groups of the BNO.[21] Formation of the BR intermediates was exothermic from −7.6 to −11.9 kcal/mol. We have studied the first step for the dimerization of the BNO **5a** (see Scheme 6). The activation energy associated with the first step of the dimerization of **5a** via **TS61** is 16.3 kcal/mol (see Table 2). Formation of the intermediate **BR2** is exothermic by −7.6 kcal/mol. The activation energy is 1.9 kcal/mol higher than that found by Houk for the dimerization of **5c**.[21] In the gas phase, **TS61** is located 3.1 kcal/mol above **TS3**.

The lengths of the forming bonds at **TS61** and **BR2** are given in Figure 3. These lengths are close to those obtained in the dimerization of **5c**.[21] At **TS61**, the BO value of the C3−C3′ forming bond is 0.31, while at the intermediate **BR2**, it is 0.99.

At the TS and intermediate associated with the first step of the dimerization of BNO **5a**, the CT between the two monomers is 0.00 e, indicating the nonpolar character of the process. The TS and intermediate involved in the dimerization mechanism have BR character. Initial $<S^2>$ values for the singlet BR stationary points, 0.13 (**TS61**) and 0.98 (**BR2**), become 0.00 (**TS61**) and 0.23 (**BR2**) after spin annihilation.[18] At the intermediate **BR2**, the atomic spin density is mainly located at O (−0.57), N (−0.44), O′ (0.57), and N′ (0.44). These values indicate that the electronic structure of this intermediate is in agreement with a BR species, where one α electron is mainly delocated at the O and N atoms belonging to one nitrile N-oxide residue, while the second β electron is localized at the O′ and N′ atoms of the other nitrile N-oxide residue.

Finally, solvent effects increase the relative energies of these BR species.[21] In dichloromethane, the activation energy for the dimerization of **5a** is 4.6 kcal/mol higher than the activation energy for the concerted formation of the [3 + 2] cycloadduct **12** (see Table 2). As a consequence, this reaction could be competitive in a minor extension. Inclusion of the solvent effects on the geometry optimization does not modify substantially the gas phase results (see Figure 3).

TABLE 3. The Valence Basin Population *N* (in e) Calculated for the ELF of Reagents, TS, "Halfway" Point on the IRC, and Zwitterionic Intermediate Involved on the Concerted and Stepwise Mechanisms for Reactions between the Benzonitrile N-Oxide 5a and 3-Methylenephthalimidines 6d

basin	5a + 6d	TS3	HWP	TS41	ZW1
		Basin Population			
V(O1)	2.61	5.68	2.81	5.76	3.29
V(O1)	3.06	–	2.68	–	2.50
V(N2,O1)	1.60	1.44	1.22	1.43	1.33
V(N2)		2.10	2.96	2.19	2.67
V(N2,C3)	2.91	1.47	3.36	1.46	2.98
V(N2,C3)	3.07	1.62	–	1.52	–
V(C3)	–	1.45	–	1.43	0.36
V(C3,C4)	–	–	1.82	–	1.80
V(C4,C5)	1.88	3.38	2.38	3.37	2.41
V(C4,C5)	1.74	–	–	–	–
V(C5,N6)	1.87	1.98	2.10	1.96	2.28
V(N6)	1.00	0.87	0.65	0.83	0.73
V(N6)	1.00	1.08	1.18	1.11	0.89

(c) Topological Analysis of the ELF of the Polar Reaction between the BNO 5a and the MPI 6d. The topology of the ELF of **TS3**, **HWP**, **TS41**, and **ZW1** was analyzed in order to obtain additional information for the electron density evolution in these reactions. The populations of the more relevant valence basins, *N*, of these structures are listed in Table 3. At **TS3**, the main changes on the population of the valence basins belonging to the BNO residue, relative to those at the reagents, are the creation of two new monosynaptic basins, V(N2) and V(C3), together with the decrease of the population of the two disynaptic basins V(N2,C3). While the creation of the monosynaptic basin V(N2) is related to the lone pair present on the N2 atom of the [3 + 2] cycloadduct **12**, the creation of the V(C3) is associated with the C3−C4 bond formation process. However, at **TS3**, there is no monosynaptic basin on the C4 carbon, which will be created in a subsequent step of the reaction and precede the creation of the disynaptic basin V(C3,C4). At **TS3**, the two disynaptic basins V(C4,C5) of **6d** are fused in a unique disynaptic basin V(C4,C5) with a population of 3.38 e. If we consider that the total population of the two disynaptic basins V(C4,C5) on **6d** is 3.63 e, we found a loss of the electron density on this fragment. On the other hand, the sum of the valence basins associated with the −CNO fragment shows an increase of the electron density on going from reagents to **TS3**.

The analysis of the valence basins of **TS41** shows a similar population to that found at **TS3**. Thus, the creation of the two new monosynaptic basins in the N2 and C3 atoms is accompanied with a decrease of the population of the valence basins V(N2,C3). As in **TS3**, there is no monosynaptic basin on the C4 carbon. The two disynaptic basins V(C4,C5) of **6d** are also fused on a unique disynaptic basin V(C4,C5). Consequently, the analysis of the topology of the ELF indicates that **TS3** and **TS41** are associated with the same electronic changes on going from the reagents to these TSs.

The more relevant changes along the stepwise pathway are found at the ZW intermediate **ZW1**. A new disynaptic basin V(C3,C4) with a population of 1.80 e is created as a consequence of the complete C3−C4 bond formation. While the population of the monosynaptic basin V(N2) increases to 0.57 e on going from **TS3** to **ZW1**, the population of the disynaptic basin V(C4,C5) decreases by 0.97 e. In addition, along the

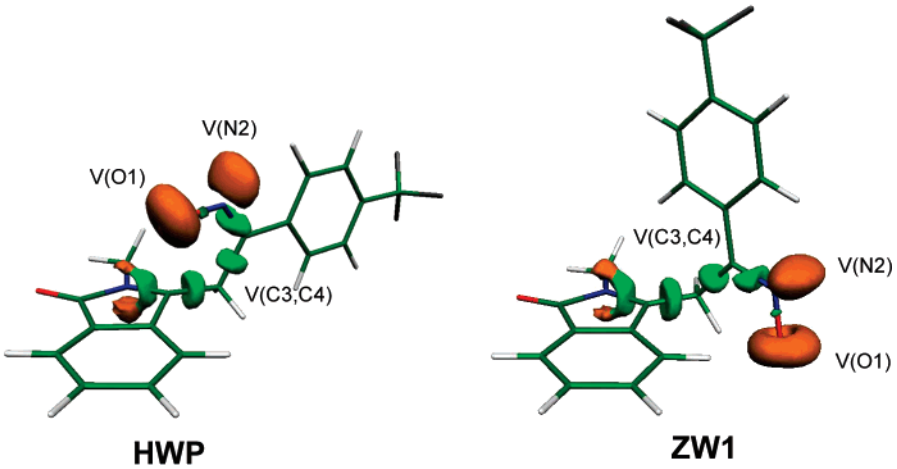

FIGURE 4. ELF localization domains ($t = 0.80$ isosurface) of the more relevant valence basins for the point **HWP** and the intermediate **ZW1** given in Table 3. This figure shows the similitude of the electronic structures of these species.

reaction path from the reagents to **ZW1**, an increase of the population of the disynaptic basin V(C5,N6) is observed: 1.87 e in **6d**, 1.96 e in **TS41**, and 2.28 e in **ZW1**. These changes point out the participation of the amide residue along the attack of the MPI **6d** to the BNO **5a**, and it explains the participation of **6d** as nucleophile in these polar cycloadditions.

The analysis of the ELF at the point **HWP** allows one to obtain some relevant information about the electronic nature of the concerted mechanism. The populations of the valence basins of **HWP** are very similar to those found at the zwitterionic intermediate **ZW1**. A representation of the ELF localization domains of the valence basins given in Table 3 for **HWP** and **ZW1** shows the similitude of the electronic structure of these species (see Figure 4). On **HWP**, there is no monosynaptic basin on the C5 atom, which will be created in a further step of the IRC and precede the creation of the disynaptic basin V(O1,C5). These behaviors assert the two-stage nature of the concerted process, where the O1−C5 bond is formed in the final step of the IRC, after completion of the C3−C4 bond formation.

The amount of CT on these processes has been evaluated by the sum of the core and valence basins belonging to the BNO **5a** and the MPI **6d** frameworks at the TSs and intermediates. These sums at the BNO framework (94.00 e) are 94.12 e at **TS3**, 94.13 e at **TS41**, and 94.45 e at **ZW1**. Therefore, there is an increase of 0.45 e for the CT along the stepwise mechanism until the formation of the intermediate **ZW1**. This CT value is very close to that obtained through the NPA, and it clearly contrasts with the negligible CT found at the BR intermediate **BR1**, 0.00 e. Along the concerted pathway, the CT at the point **HWP** is 0.34 e. Therefore, although both **TS3** and **TS41** present a low CT, probably as a consequence of the early character of these TSs, along the attack of MPI **6d** to BNO **5a**, there is an increase of the CT associated with the nucleophile/electrophile interaction until the formation of the C3−C4 bond.

(d) Study of the Reaction between 2,4,6-Trimethylbenzonitrile N-Oxide 5f and Acrolein 15. Reactions toward Electron-Deficient Dipolarophiles. Reaction Model III. Finally, in order to generalize this study, the channels associated with the 13DC reaction and oxime formation on the reaction of BNOs with electron-deficient dipolarophiles was considered. Thus, the reaction between 2,4,6-trimethylbenzonitrile N-oxide **5f** and acrolein **15** was studied as a reaction model (see Scheme 7). Two reactive channels were considered. They are related to the dihedral angle formed between the π C−N bond of BNO and the π C−C bond of acrolein along the C−C bond formation, which takes the values of 0 and 120°. These channels are named *channel 1* and *2*, allowing the concerted formation of the [3 + 2] cycloadduct **16** and the stepwise formation of the oxime **17**. Three TSs, **TS7**, **TS81**, and **TS82**, one BR intermediate, **BR3**, one [3 + 2] cycloadduct, **16**, and one oxime, **17**, were located and characterized (see Scheme 7).

SCHEME 7

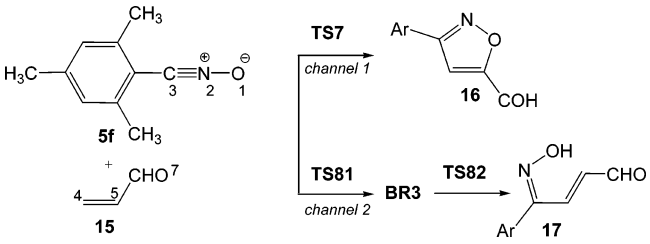

TABLE 4. (U)B3LYP/6-31G* Relative Energies (ΔE, in kcal/mol, relative to 5f + 15), in the Gas Phase and in Dichloromethane, of the Stationary Points for the Concerted and Stepwise Reactions between the 2,4,6-Trimethylbenzonitrile N-Oxide 5f and Acrolein 15

	gas phase	dichloromethane
TS7	13.7	14.3
16	−29.1	−28.0
TS81	22.6	24.3
BR3	14.2	16.2
TS82	27.1	29.2
17	−19.3	−21.2

The activation energies associated with the reaction of BNO **5f** with acrolein **15** along *channels 1* and *2* are 13.7 (**TS7**) and 22.6 (**TS81**) kcal/mol; formation of the corresponding intermediate **BR3** is endothermic, 14.2 kcal/mol (see Table 4). It is interesting to remark that the first step in the formation of the oxime **17** needed open shell calculations in order to find **TS81** and **BR3** as stationary points on the PES. The activation energy associated with the concerted cycloaddition via **TS7** is closer to that obtained by Houk for the reaction between the BNO **5f** and methyl propiolate, 13.4 kcal/mol.[22] Finally, the activation energy for the hydrogen abstraction at **BR3** via **TS82** is 12.9

(22) Hu, Y.; Houk, K. N. *Tetrahedron* **2000**, *56*, 8239−8243.

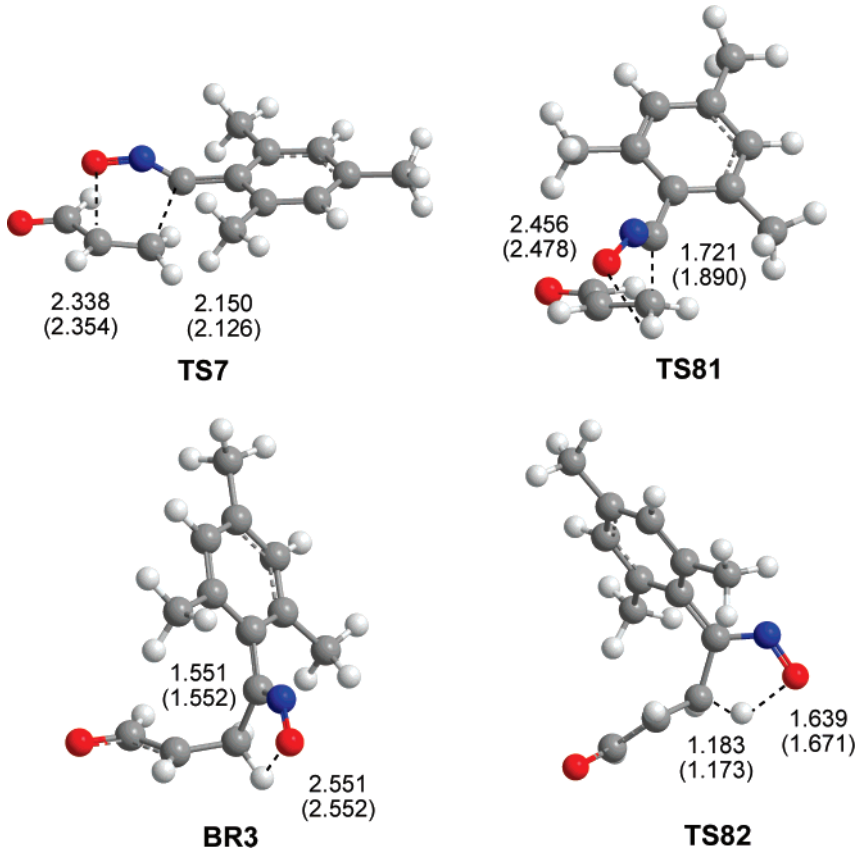

FIGURE 5. Structures of the transition states and biradical intermediate involved in the concerted and stepwise reaction pathways between 2,4,6-trimethylbenzonitrile N-oxide **5f** and acrolein **15**, reaction *Model III*. The distances are given in angstroms. Values in parentheses correspond to the geometries in dichloromethane.

kcal/mol. For the reaction *Model III*, this is the rate-determining step for the formation of the oxime **17**, with activation energy of 27.1 kcal/mol. This activation energy is 13.3 kcal/mol higher in energy than that for the formation of the [3 + 2] cycloadduct **16**. This large energy difference prevents the formation of the oxime **17**. Formation of the cycloadduct **16** and the oxime **17** is exothermic by −29.1 and −19.3 kcal/mol.

The lengths of the forming bonds at the TSs and intermediate are given in Figure 5. The lengths of the C3−C4 and O1−C5 forming bonds at concerted **TS7** are closer to those found at the TS associated with the reaction between the BNO **5f** and methyl propiolate (2.164 and 2.381 Å).[22] At **TS82**, the lengths of the C4−H4 breaking and O1−H4 forming bonds indicate that the hydrogen transfer process is more delayed than that at **TS22**. The N2−C3−C4−C5 dihedral angles at **TS7** and **TS81**, which define the approach mode of BNO **5f** to acrolein **15**, are −3.8 and 94.1°. The deviation of the dihedral angle at **BR3** from 120° (84.9°), together with the O−H distance (2.55 Å), indicates that there is no hydrogen bond at this intermediate.

At the concerted **TS7**, the BO values of the C3−C4 and O1−C5 forming bonds are 0.35 and 0.20. These BO values indicate that this concerted TS corresponds with an asynchronous bond formation process, where the C−C bond formation at the β-position of the acrolein **15** is more advanced than the O−C one. At **TS81**, the BO value of the C3−C4 forming bond is 0.49, while this value at **BR3** is 0.83. Finally, at **TS82**, the BO values at the C4−H4 breaking and O1−H4 forming bonds are 0.66 and 0.18.

The CT along the reaction between the BNO **5f** and acrolein **15** was evaluated at the BR intermediate **BR3**. The sum of the natural charges at the electron-deficient acrolein framework at **BR3** is −0.01 e. On the other hand, the amount of CT evaluated using the ELF of **BR3** at the acrolein fragments is −0.07 e. The negligible CT at this intermediate points to a very low polar process, despite the electrophile character of acrolein (see later). Therefore, while the reactions involving electrophilically activated BNOs have some polar character, the reactions involving electrophilically dipolarophiles have a nonpolar character.

The **TS81** and the intermediate **BR3** involved at the stepwise mechanism have a BR character. Initial $<S^2>$ values for the singlet BR stationary points, 0.68 (**TS81**) and 0.86 (**BR3**), become 0.06 (**TS1**) and 0.09 (**BR3**) after spin annihilation.[18] At the intermediate **BR3**, the atomic spin density is mainly located at O1 (−0.53), N2 (−0.42), C5 (0.75), and O7 (0.34). These values indicate that the electronic structure of this intermediate is in agreement with a BR species, where one α electron is mainly delocated at the O1 and N2 atoms belonging to the NBO **5f** residue, while the second β electron is localized on the C5 and the carbonyl O7 atoms belonging to the acrolein residue.

Finally, in dichloromethane, all species are stabilized between 4 and 10 kcal/mol. The reagents are more stabilized than the concerted **TS8**. As a consequence, in solution, the activation energy for the 13DC increases to 14.3 kcal/mol.[22] The lesser solvated species is the intermediate **BR3**, 6.3 kcal/mol, as a consequence of the low polar character of the this species. Note that the zwitterionic intermediate **ZW1** is stabilized by 11.5 kcal/mol. In dichloromethane, the stepwise formation of the oxime **17** remains 14.9 kcal/mol more energetic than formation of the [3 + 2] cycloadduct **16** (see Table 4). Inclusion of the solvent

TABLE 5. Electronic Chemical Potential (μ, in au), Chemical Hardness (η, in au), and Global Electrophilicity (ω, in eV) of Fulminic Acid 1, Ethylene 2, Benzonitrile N-Oxides 5, and 3-Methylenephthalimidines 6

compound	μ	η	ω
5a (Ar = 4-$CF_3C_6H_4$)	−0.1590	0.1775	1.94
5e (Ar = 2,6-$Cl_2C_6H_3$)	−0.1568	0.1761	1.90
acrolein (**15**)	−0.1610	0.1922	1.84
5b (Ar = 3-$CF_3C_6H_4$)	−0.1549	0.1827	1.79
6a (*X* = 3-$CF_3C_6H_4$)	−0.1467	0.1638	1.79
5g (Ar = 2,6-$F_2C_6H_3$)	−0.1504	0.1807	1.70
5c (Ar = 4-ClC_6H_4)	−0.1490	0.1784	1.69
6b (X =C_6H_5)	−0.1374	0.1619	1.59
6c (X = $CH_2C_6H_5$)	−0.1394	0.1674	1.58
6d (X = CH_3)	−0.1392	0.1679	1.57
5d (Ar = C_6H_5)	−0.1406	0.1847	1.46
5f (Ar = 2,4,6-$Me_3C_6H_2$)	−0.1311	0.1791	1.31
fulminic acid (**1**)	−0.1249	0.2919	0.73
ethylene (**2**)	−0.1239	0.2855	0.73

effects on the geometry optimization does not modify substantially the gas phase results (see Figure 5). In dichloromethane, the length of the C3−C4 forming bond at **TS81** increases to 0.169 Å as a consequence of the stabilization of this energetic TS.

(e) Global Electrophilicity Analysis. Recent studies carried out on DA[23] and 13DC[24] reactions with a polar character have shown that the indexes defined within the DFT[25] are powerful tools to study their reactivity. In Table 5, the static global properties, electronic chemical potential (μ), chemical hardness (η), and global electrophilicity (ω) of fulminic acid, **1**, ethylene, **2**, the BNOs **5**, and the MPIs **6** are presented. Some of the electrophilically activated BNOs used experimentally in 13DC reactions are included in this table.

The value of the electronic chemical potential of fulminic acid **1**, −0.1249 au, is closer to that for ethylene **2**, −0.1239 au. Therefore, along the 13DC between **1** and **2**, none of them will have any trend to provide electron density to the other, and a nonpolar 13DC will be expected. On the other hand, for the experimental models, the electronic chemical potential of the BNO **5a** (Ar = 4-$CF_3C_6H_4$), −0.1590 au, is higher than that for MPI **6c** (Y = $CH_2C_6H_5$), −0.1394 au, thereby indicating that along a polar process the net charge transfer will take place from **6c** to **5a**, in clear agreement with the NPA and the ELF analyses.

Fulminic acid **1** and ethylene **2** have identical low electrophilicity values, 0.73 eV; both reagents are classified as marginal electrophiles.[24a] Therefore, it will be expected that they react through a nonpolar 13DC. Benzonitrile N-oxide **5d** (Ar = C_6H_5) has an electrophilicity value of ω = 1.46 eV, being classified as a strong electrophile.[24a] Substitution of the hydrogen atom of fulminic acid **1** by a phenyl group on **5d** increases notably its electrophilicity. Inclusion of three electron-releasing methyl groups on the phenyl substituent decreases the electrophilicity of **5f** (Ar = 2,4,6-$Me_3C_6H_2$) to 1.31 eV, being the poorest electrophile of the BNO series given in Table 5. On the other hand, the inclusion of an electron-withdrawing (EW) group at the *para* position or two groups on the *meta* positions of the phenyl group raises the electrophilicity of the BNOs. Some electrophilically activated 4-substituted and 2,6-disubstituted BNOs are listed in Table 5. The electrophilicity of the BNOs increases with the EW character of the substituents: 1.69 eV **5c** (Ar = 4-ClC_6H_4), 1.70 eV **5g** (Ar = 2,6-$F_2C_6H_3$), 1.79 eV **5b** (Ar = 3-$CF_3C_6H_4$), 1.90 eV **5e** (Ar = 2,6-$Cl_2C_6H_3$), and 1.94 eV **5a** (Ar = 4-$CF_3C_6H_4$). Some conclusions can be drawn from this series: (i) the electrophilicity of these EW-substituted BNOs is larger than that for benzonitrile N-oxide **5d**; (ii) for the *para*-substituted subseries, the increase of the electrophilicity in the order Cl < CF_3 is in agreement with the EW character of the substituent; (iii) for the CF_3-monosubstituted derivatives, the substitution on the 4-position, **5a**, gives the BNO an electrophilicity that is larger than that of the substitution on the 3-position, **5b**; and (iv) for the chlorine derivatives, the 2,6-disubstitution, **5e**, produces a large increase of the electrophilicity than it does at the 4-substitution, **5c**.

The electrophilicity of the MPI model **6d** (Y = CH_3), ω = 1.57 eV, is closer to that for the experimental molecule **6c** (Y = CH_2Ph), ω = 1.58 eV; therefore, they are classified as strong electrophiles. These large values are a consequence of the presence of the amide framework on the MPIs **6**. Substitution of the N-methyl or N-benzyl groups by a phenyl group, **6b**, or a 3-$CF_3C_6H_4$ group, **6a**, increases the electrophilicities of the MPI to 1.59 and 1.79 eV, as a consequence of the delocation of the nitrogen lone pair on these phenyl substituents. This increase of the electrophilicity, which can be related to a decrease of the nucleophilic character of these MPIs, could explain the experimental observation that for **6b** (X = C_6H_5) and **6a** (X = 3-$CF_3C_6H_4$) formation of the corresponding oximes were not observed,[8] indicating that in these cases the stepwise pathway is not competitive with the concerted 13DC reactions.

Recently, the DA reactions between electron-deficient reagents (dienes and dienophiles) have been studied within the DFT framework.[26] We have shown that, along a polar cycloaddition, the reagents located at the top of the electrophilicity scale force the reagents located below them to behave as nucleophiles. Therefore, along the 13DC reaction between the BNO **5a** (Ar = 4-$CF_3C_6H_4$) and the MPI **6d** (X = CH_3), it would be expected that the net charge fluxes from **6d** acting as nucleophile to the BNO **5a** acting as electrophile. Note that fulminic acid **1** and ethylene **2** have low electrophilicity values, and as a consequence, neither of them will act as a strong electrophile in a polar cycloaddition. This analysis is in complete agreement with the CT found along the reaction between the BNO **5a** and the MPI **6d** based on the NPA and ELF analyses.

Finally, it is interesting to remark that despite the electrophilicity difference between the BNO **5f**, ω = 1.31 eV, and acrolein **15**, ω = 1.84 eV, the process has a very low polar character. Note that acrolein should act as electrophile along polar interactions. This indicates that these BNOs will not have any tendency to act as nucleophiles in polar reactions.

Conclusions

The reaction mechanisms of fulminic acid and benzonitrile N-oxides toward ethylene, 3-methylenephthalimidines, and acrolein with formation of [3 + 2] cycloadducts and oximes have been studied using density functional theory (DFT) at the (U)B3LYP/6-31G* level. The analysis based on the natural bond

(23) (a) Domingo, L. R.; Aurell, M. J.; Pérez, P.; Contreras, R. *Tetrahedron* **2002**, *58*, 4417−4423. (b) Domingo, L. R.; Aurell, M. J.; Pérez, P.; Contreras, R. *J. Phys. Chem. A* **2002**, *106*, 6871−6875.

(24) (a) Pérez, P.; Domingo, L. R.; Aurell, M. J.; Contreras, R. *Tetrahedron* **2003**, *59*, 3117−3125. (b) Aurell, M. J.; Domingo, L. R.; Pérez, P.; Contreras, R. *Tetrahedron* **2004**, *60*, 11503−11509.

(25) Geerlings, P.; De Proft, F.; Langenaeker, W. *Chem. Rev.* **2003**, *103*, 1793−1873.

(26) Domingo, L. R. *Eur. J. Org. Chem.* **2004**, 4788−4793.

orbital (NBO) and the topological analysis of the electron localization function (ELF) at the TSs and intermediates explains correctly the electronic nature, biradical (BR) or zwitterionic (ZW), of these reactions. Energies, geometries, and electronic structures of all species involved in the two competitive pathways have been analyzed in order to explain the experimental outcomes. Some conclusions can be obtained from the present study:

(i) For these 13DC reactions, both BR (*Models I* and *III*) and ZW (*Model II*) concerted mechanisms have similar energies. The activation energy for the *Model II* is slightly higher than that for the *Model I*.

(ii) Whereas for the reaction *Models I* and *III* the activation energies associated with the oxime formation via BR stepwise pathways are 7.6 and 13.3 kcal/mol higher in energy than that for the concerted one, for the *Model II*, with a large polar character, this difference is only 0.5 kcal/mol. As a consequence, only for the reaction *Model II*, formation of the oximes is competitive with the concerted pathway.

(iii) Formation of the oximes **4** and **17** (*Models I* and *III*) and the oxime **12** (*Model II*) has different mechanisms as a consequence of the electronic nature of the corresponding intermediates. While the conversion of the BR intermediates **BR1** and **BR3** into **4** and **17** involves a hydrogen transfer process, the conversion of the ZW intermediates **ZW1** and **ZW2** into **13** involves a proton transfer process.

(iv) At the reaction *Model II*, the barriers for the proton transfer processes present a very low value, 1.7 and 1.4 kcal/mol. As a consequence, the conversion of the intermediates **ZW1** and **ZW2** into the [3 + 2] cycloadduct **12** via a C3−C4 bond rotation is not competitive. Note that the barriers for the hydrogen abstraction at the intermediates **BR1** and **BR3** are 9.2 and 12.9 kcal/mol.

(v) While the earlier hydrogen bond formation at the polar stepwise pathways of the reaction *Model II* favors the nucleophilic attack of the MPIs to the electrophilically activated BNOs, the positive charge that develops at the nucleophilic ethylene increases the acid character of the C−H bond, favoring the subsequent proton abstraction. As a consequence, the hydrogen bond formation favors both the C−C bond formation and the proton transfer process. Note that, for the addition of amines to nitrile N-oxides, formation of the corresponding amidoximes takes place along a concerted process.[27]

(vi) Analysis of the channel associated with the oxime formation in the reactions of BNOs with acrolein reveals that formation of oximes is not competitive with the 13DC reactions. The low charge transfer found in these reactions points out the nonparticipation of the BNOs as nucleophiles toward electrophilically activated ethylenes.

Overall, the results of our study allow us to state that the use of electrophilically activated nitrile N-oxides toward electron-rich ethylenes changes the mechanism of the reaction from biradical to a zwitterionic character. At these polar processes, the formation of zwitterionic intermediates could be competitive to the concerted 13DC, allowing the formation of the corresponding oximes. In these cases, both the 13DC reaction and the oxime formation are characterized by the initial nucleophilic attack of an electron-rich C−C double bond of the dipolarophile to the electrophilically activated carbon atom of the nitrile N-oxide. The use of the electrophilicity index of the reagents has been revealed to be an effective tool for predicting the polar nature of these reactions.

Acknowledgment. This work was supported by research funds provided by the Ministerio de Ciencia y Tecnología of the Spanish Government by DGICYT (project BQU2002-01032) and the Universidad de Valencia (project UV-AE-06-3). J.A.S. thanks the Ministerio de Ciencia y Tecnología for his doctoral fellowship.

Supporting Information Available: Computational methods; UB3LYP/6-31G*, CCSD(T)/6-31G*, and BD(T)/6-31G* total energies of the stationary points for the reactions between fulminic acid **1** and ethylene **2**; (U)B3LYP/6-31G* total energies, in gas phase and in dichloromethane, of the stationary points for the reactions between **5a** and **6d**, the first step of the dimerization of **5a**, and for the reactions between **5f** and **15**. Unique imaginary frequency of TSs, and (U)B3LYP/6-31G* Cartesian coordinates of all structures. This material is available free of charge via the Internet at http://pubs.acs.org.

JO0613986

(27) Nguyen, M. T.; Malone, S.; Hegarty, A. F.; Williams I. I. *J. Org. Chem.* **1991**, *56*, 3683−3687.